Applied Biochemistry and Biotechnology (2024) 196:949–970
https://doi.org/10.1007/s12010-023-04571-1

ORIGINAL ARTICLE

Nanoemulsion-Based System as a Novel and Promising Approach for Enhancing the Antimicrobial and Antitumoral Activity of *Thymus vulgaris* (L.) Oil in Human Hepatocellular Carcinoma Cells

Simran Nasra[1] · Nikita Meghani[1] · Ashutosh Kumar[1]

Accepted: 24 May 2023 / Published online: 5 June 2023

Abstract

The utilisation of medicinal plants and their essential oils is receiving more attention due to the ineffectiveness of current therapeutic methods in the treatment of various cancers and the rising incidence of bacterial antibiotic resistance. Thymol, an active ingredient of *Thymus vulgaris*, is known to have hepatoprotective, antibacterial, and antioxidant properties. To overcome major obstacles to their usage, such as quick oxidation and high volatility, plant essential oils must be administered through a system to improve the delivery of their active pharmaceutical ingredient. The bioavailability of active substances may be enhanced by the colloidal dispersion nanoemulsion. Therefore, this study aims to derive a comparative evaluation of the thyme oil nanoemulsion formulation and the characterisation of its antibacterial and antitumorigenic activities. A nanoemulsion (NE) with a droplet size of 122.2 ± 1.079 nm was discovered to be stable and mono-dispersed for 4 months and inhibited the growth of *B. subtilis*, *E. coli*, *P. aeruginosa*, and *S. aureus*. It also displayed antitumorigenic capabilities in HepG2 cells by arresting the cell cycle in the G2/M phase and upregulating the gene expression levels of Bcl-2-associated X protein (Bax), Caspase 3, 8, and 9, as well as a concomitant concentration-dependent decrease in B-cell leukaemia/lymphoma 2 protein (BCL2). Along with an increase in inducible nitric oxide synthase (iNOS) levels, upregulation of the expression levels of the reactive oxygen species (ROS), mitogen-activated protein kinase (MAPK), and endoplasmic reticulum (ER) stress pathways was also seen, indicating of ROS formation in the cancer cells.

Keywords Thyme nanoemulsion · Antimicrobial · Hepatoprotective and antitumorigenic

✉ Ashutosh Kumar
ashutosh.kumar@ahduni.edu.in

[1] Biological and Life Sciences, School of Arts & Sciences, Ahmedabad University, Central Campus, Navrangpura, Ahmedabad 380009, Gujarat, India

Introduction

Food-borne infections are a significantly escalating public health and economic concern [1]. According to estimates, 30% of people in industrialised nations experience a food-borne illness each year, and 25% of all foods produced worldwide are lost to microbial spoilage [2, 3]. According to reports, synthetic antioxidants and antimicrobials should be avoided owing to their toxicity, their potential for cancer, and environmental hazards. As a result, natural goods are being examined rather than synthetic ones [4]. Essential oils are potential antimicrobial agents for food preservation because they have the ability to combat a number of pathogenic agents transmitted by food and microorganisms responsible for food deterioration [5, 6]. The ability of essential oils to stop the growth of numerous types of microbes in food items, including *Salmonella* sp., *E. coli* [7], *Bacillus* sp., *Listeria* sp., [8], and *Aspergillus* sp., [9], has been confirmed in multiple studies about their antimicrobial action.

The essential oil extracted from thyme (*Thymus vulgaris*) is one of the most studied and used because of its antibacterial qualities [10–12]. Thyme oil possesses a variety of pharmacological qualities, such as antioxidant, antiinflammatory, and antineoplastic effects [13]. The presence of the phenolic hydroxyl group in thymol (2-isopropyl-5-methyl phenol), a significant essential oil component (EOC), may have provided for its antibacterial activity [14]. Thymol has also been given the "Generally Recognized as Safe" (GRAS) label by the US Food and Drug Administration for use as an additive in the food [15]. Thyme is known for its potent antimicrobial and antioxidant properties, which are due to the presence of a variety of bioactive compounds such as thymol, carvacrol, p-cymene, and linalool [16]. Recently, thyme nanoemulsions have gained considerable attention in the field of nanotechnology due to their potential therapeutic applications in the treatment of infectious diseases and cancer [17, 18] and also has been reported to exhibit antimicrobial activities against *Salmonella senftenberg* [19, 20], *Salmonella enteritidis* [21], *Micrococcus luteus*, *L. monocytogenes*, *Enterococcus* spp., and *Aeromonas* spp. [22].

Thyme's biodegradable, powerful antibacterial, and antioxidant properties have made it a target for much wider use in the food and agriculture industries [23]. Its limited water solubility, however, restricts its use in aquatic media and lowers its biological activity [24]. Additionally, the physical and chemical instability of lipophilic bioactive chemicals, such as thymol, in the presence of oxygen, light, and temperature diminishes their efficacy [25, 26]. By creating thymol nanoemulsions and entrapping them in appropriate surfactants to create nanodroplets, these issues may be resolved [27, 28]. Thymol becomes physically and chemically stable in the aqueous media as a result of its encapsulation [29]. Nanoemulsion (NE) techniques have been suggested as a solution to these drawbacks because they enhance chemical stability during storage, augment the dispersal of essential oil in aqueous constructions, minimise the alteration of sensory processes, and in certain instances, enhance their antimicrobial action [30]. Nanostructures may encourage inert cellular absorption devices because of their tiny particle size, which lowers mass transfer and boosts antimicrobial action [31]. The monoterpenoid phenols carvacrol and thymol in particular, which have a lot of potential to be used in therapeutic and management interventions against cancer due to their pharmacological characteristics, are among the active ingredients found in thyme. Thyme oil NE is also said to have antineoplastic properties [32, 33]. Carvacrol and thymol had anticancer effects in a range of cell lines that closely resembled human tumours, demonstrating their potential as chemo-preventive or anticancer medicines in numerous kinds of malignancies [34]. Some of the primary mechanisms

of thyme's anticancer actions include inducing apoptosis, inhibiting cell growth, increasing ROS production, depolarising the mitochondrial membrane, activating Bax pro-apoptotic mitochondrial proteins, inhibiting angiogenesis, interacting with caspase or poly-ADP ribose polymerase, and reducing tumorigenesis by regulating the activity of carcinogen metabolising enzymes [33, 35]. This study's primary objectives were to develop and characterise thyme oil nanoemulsions, determine their stability over time and under various conditions, and evaluate their potential cytotoxicity, antibacterial, and antitumour properties. There are currently no reports on the use of thyme nanoemulsion as a potential therapy for liver cancer, and this study indicates that it has a superior anticancer effect when compared to conventional thyme extract. This is the first study to report that thyme nanoemulsion inhibited hepatocellular carcinoma cell growth by triggering programmed cell death along with known antimicrobial properties that warrant further investigation, which has the potential to improve patient outcomes and quality of life.

Materials and Methods

Chemical Reagents

Thymus vulgaris wood-derived essential oil, with a purity level of 99.9%, was bought from Devinez, India. The source of Tween 80 was Sigma-Aldrich in India. Phosphate buffer saline (PBS) and propidium iodide were purchased from HiMedia Laboratory Pvt. Ltd., India. Throughout the course of the investigation, deionised and Milli-Q (Millipore Corporation) water was utilised for all assays. The primers were obtained from Eurofins Genomics LLC.

Nanoemulsion Preparation

The hydrophilic-lipophilic balance (HLB) value of Tween 80 is 15, which is very high, hence was selected for the synthesis of oil-in-water nanoemulsion. Thyme oil was prepared as an oil-in-water form of nanoemulsion at various concentrations using 0.5% of Tween 80 [36]. Initially, thyme oil was mixed with 100% ethanol at an equal ratio and different concentrations of Tween 80. This consisted of the organic phase, which was first thoroughly mixed and then heated at 86 °C. After an hour of heating, the water was added to the organic phase to form a coarse emulsion. The coarse emulsion was then treated to ultrasonic emulsification using a 20 kHz Sonicator after being agitated for 30 min at 400 rpm on a magnetic stirrer (Sonics, Vibra Cell). Sonication was done with a sonotrode that had a 5-mm probe diameter, a power output of 130 W, and a 75% amplitude. Sonication was carried out for different time points: 10 min, 20 min, and 30 min and all the synthesised nanoemulsions were cooled and then characterised and further assessed for their stability.

Characterisation of Nanoemulsion

Hydrodynamic Size and Zeta Potential

To prevent any measurement difficulties due to the viscosity of the nanoemulsion components and to reduce the multiple scattering effects, thyme nanoemulsion was dispersed in

Milli Q water at a concentration of 10% [37]. Using a Zetasizer Nano-ZS with a 4.0 mW, 633-nm laser, 1 mL of nanoemulsion suspension was placed into a disposable polystyrene cuvette to calculate the hydrodynamic size and zeta potential (Model ZEN3600, Malvern Instruments, Malvern, UK).

Physiochemical Characterisation

Using a calibrated pH meter and the Zetasizer Nano-ZS, the pH and electrical conductivity (σ) of all the formulations were quantitatively examined (Model ZEN3600, Malvern Instruments, Malvern, UK).

Stability of Nanoemulsions

All of the formulations were submitted to the following circumstances in order to evaluate the stability of NE. If phase separation was not noticed at any stage, the nanoemulsion was deemed stable. The formulations were centrifuged for 30 min at 10,000 rpm to check for any phase separation. For the heating-cooling cycle, all the synthesised formulations were kept at 40 °C and 4 °C alternatively for 24 h each. Similarly, for freeze-thaw stress, nanoemulsions were kept at 20 °C and 2 °C alternatively for 24 h each and the cycle was repeated thrice. The nanoemulsion used for further studies was kept at room temperature to assess the stability for a longer period. The hydrodynamic size was observed every month for the next 4 months.

Antibacterial Activity of Thyme Nanoemulsion

Bacterial Strains and Growth Conditions

The bacterial strains were obtained from Microbial Type Culture Collection and Gene Bank (MTCC). The strains selected for the present study were *Bacillus subtilis* (MTCC 10073), *Escherichia coli* (MTCC 1687), *Staphylococcus aureus* (MTCC 1430 T), and *Pseudomonas aeruginosa* (MTCC 1934 T) and were grown in a nutrient broth (NB). Bacterial stocks were kept in nutritional broth containing 30% (vol/vol) glycerol at − 80 °C. The freshly made nutrient broth was inoculated with aliquots from stock culture, which was then cultivated at 37 °C overnight. Each study's original culture of bacteria had an optical density (OD) between 0.12 and 0.14 at 600 nm. The CFU of bacterial culture was standardised using nutrient agar.

Microbial Growth Inhibition

Using growth inhibition tests, the bactericidal efficacy of thyme oil and nanoemulsions was studied. One percent of the primary culture was added to the new nutrient broth for the antibacterial experiment, which was then incubated at 37 °C for 1 h. The experiment was carried out on a 96-well culture plate, where the bacteria were initially infected, followed by the addition of the appropriate treatments, with a final volume of 100 µL in each well. The nutrient broth was utilised as the control, and for the oil tests, 2.5% oil was supplemented to each well. Similarly, in the comparison trials, 0.5% of Tween 80 and 1% of Triton X were used. The nutrient broth was used to make all of the treatments. As a positive control, Triton X was employed. Each well's OD was maintained between 0.13 and 0.14 at 600 nm (1×10^8 CFU/mL of bacteria equal to an OD of 0.139). By monitoring the absorbance @ 600 nm using a SYNERGY-HT multiwell plate reader (Bio-Tek, USA) and the Gen5 software, the bacterial growth was tracked for 24 h.

Assessment of MBC and MIC

MIC and MBC were executed as previously described by Moghimi et al. [38]. In brief, 180 µL of nanoemulsion and 20 mL of bacterial culture with an OD of 0.12 to 0.14 at 600 nm were added to each well of a 96-well plate before being serially diluted in nutritional broth. The maximum dilution demonstrating no bacterial growth was utilised to estimate the MIC after the plates were incubated at 37 °C overnight. MBC was calculated by plating 100 µL of bacteria culture from wells that had no visible signs of growth on the nutrient agar and allowing it to sit at 37 °C overnight. The maximum dilution, MBC, exhibits a 99.9% reduction in the total number of bacterial cells. Negative controls included nutrition broth, and positive controls included 1% Triton X.

Trypan Blue Staining Assay

Trypan blue assays were used to examine cell viability. In a nutshell, 1% of the initial culture was transferred into a new nutrient broth and incubated at 37 °C for 1 h. Five milliliters of bacterial solution was incubated for 1 h with 5 mL of NE, 2.5% thyme oil, 0.5% Tween 80, and 1% Triton X. The control was the nutritional broth. The bacterial solution was centrifuged for 10 min at 4000 rpm after 1 h, and the pellet was then resuspended in 1 mL of PBS. The findings were also contrasted with fenugreek nanoemulsion, whose antibacterial properties are widely known. An equivalent volume of bacterial solution was incubated with 0.2% trypan blue dye and carefully mixed to determine the viability count. Ten microliters of the mixed solution was used to measure the number of live cells after it had been at room temperature for 2–3 min. The data is presented as percent viability.

$$\% \text{ Viable cells} = \left(\frac{\text{Number of viable cells}}{\text{Number of total cells}}\right) \times 100$$

Membrane Permeability Assay

Briefly, 1% of the primary culture was added to the new nutrient broth and cultured at 37 °C for 1 h. At 600 nm, the culture's OD was 0.12 to 0.14. The 1-, 10-, and 100-fold diluted and undiluted nanoemulsion and oil, together with nutritional broth as a reference, 0.5% Tween 80, and 1% Triton X, were all incubated with the bacterial suspension for 1 h. One percent of Triton X was taken as a positive control. The sample was then centrifuged for 10 min at 5000 rpm, and the supernatant was read using a UV-Visible Spectrophotometer at 260 nm. Fold leakage is described as an increase in permeability.

Anticancer Property of Thyme Nanoemulsion

MTT Assay

The human hepatocellular carcinoma cell line Hep G2 was obtained from the National Center for Cell Sciences (NCCS), Pune, India. Hep G2 cells were cultured in CO2 incubators at 37 °C in Eagle's Minimum Essential Media (MEM) with a humidified environment containing 5% CO2. Ten percent of heat-inactivated FBS, 0.2% of sodium bicarbonate, and

10 mL/L of an antibiotic and the antifungal solution were added to the medium as supplements. In 96-well plates, cells were seeded at a density of 10,000 cells/well for the cell viability experiment. Thyme nanoemulsion (concentrations of 25, 50, 100, 150, 200, 250, 300, and 400 μM) was applied to the cells after 24 h. After that, the plates were incubated for 6 and 12 h at 37 °C. After adding 20 L of MTT solution (5 mg/mL) to each well, the cells were cultivated for an additional 4 h. Additionally, the medium was removed, and DMSO was used to dissolve the formazan crystals. Using a microplate reader at 490 nm, the optical density was read (Biotek, Synergy H1). By comparing the rates of cell growth with control cells, calculations were made.

Cell Cycle Analysis

Different NE concentrations (25, 50, 100, and 200 μM) were applied to Hep G2 cells that had been plated on a 6-well plate for 24 h. Following the procedure, the media were evacuated into separate tubes, and cells were collected and preserved in 70% ethanol (at 22 °C for 30 min). Following fixation, cells were lysed in 1 mL of PBS with 0.2% Triton X 100 for 30 min at 40 °C. Centrifugation was used to pellet the cells, which were then re-suspended in 500 mL of PBS with 20 mL RNAse (10 mg/mL) for 30 min at 370 C. Finally, cells were stained for 10–15 min at 40 C with 10 mL propidium iodide (1 mg/mL) in PBS before being examined on a flow cytometer (FACS Calibur, BD Biosciences, CA).

Mitochondrial Membrane Potential Measurement

For 24 h, nanoemulsions were applied to Hep G2 cells at various dilutions of 1:1, 1:10, and 1:100 to evaluate any changes in the potential of the mitochondria (MMP). The rise in green bloom shows that the apoptotic pathway is being activated by mitochondria. Since the mitochondria house the cells' electron transport system, any disturbance in the MMP can affect cellular respiration and metabolism, suggesting activation of the intrinsic route. The alteration in mitochondrial membrane potential was measured using the lipophilic cationic dye JC-1. When a decrease in mitochondrial membrane potential is noticed, the JC-1 dye is well recognised for reversibly changing colour from red to green fluorescence. Briefly, 3×105 cells/well in a 6-well plate were seeded, allowed to develop for 24 h, and then exposed to nanoemulsions for an additional 24 h. As a positive control, Camptothecin (1 M) was utilised. After the treatment was stopped, cells were rinsed with PBS and exposed to 10 M JC-1 dye for 15 min at 37 °C. A BD FACS Calibur flow cytometer was used to analyse the cells.

RNA Isolation and RT-PCR Studies

TRIzol reagent was used to extract total RNA from control and thyme nanoemulsion treated (25, 50, 100, 200 M) Hep G2 cells (Life Technologies). A high-capacity cDNA reverse transcription kit was used to create the cDNA (Applied Biosystems). The 20-μL reaction mixture for real-time included 10 μL of the 23 master mix (23 RT Buffer (2 μL), 0.8 μM dNTP Mix (0.8 μL), random primers (2 μL), RNase Inhibitor (1 μL), 1 μL multiscribe reverse transcriptase (RT), and 3.2 μL nuclease-free H2O), as well as an equivalent proportion of the diluted RNA sample. Thermal cycling at 25 °C for 10 min, 50 °C for 15 min, 85 °C for 5 min, and 4 °C pausing was employed to carry out the RT response. A 25-μL volume containing 100 ng cDNA, 100 μL dNTPs, 2.5 mM MgCl2, 1 unit DNA polymerase

(Thermo Scientific), and 1 µL gene-specific forward and reverse primers were used to conduct the RT-PCR. The results of 30 cycles of PCR amplification were examined.

Statistical Analysis

The mean and SEM were used to summarise the findings of three different investigations, each of which was conducted in triplicate. For statistical analysis, a one-way ANOVA with paired, two-tailed Student's *t*-tests were utilised ($P < 0.01$, $P < 0.001$, and $P < 0.0001$ indicate significant differences from the control).

Results and Discussion

Characterisation of Nanoemulsion

A thorough characterisation is required in order to comprehend the occurrence at the nano-biointerface. Characterisation of nanoemulsion shed light on the relationship between the interfacial properties and the overall characteristics of nanoemulsions, as well as how these interfacial properties depend on the type, concentration, and characteristics of the surface-active components present in the nanoemulsion system or on external factors like pH, ionic strength, and temperature [39].

Droplet Size and Zeta Potential Measurement

Colloidal interactions between two neighbouring droplets in nanoemulsions depend on the droplet size and are caused by attractive interactions like Van der Waals, hydrophobic bonds, and repulsive interactions like electrostatic and stearic bonds between them. The increase in the oil phase concentration at a certain surfactant concentration also has an impact on the size of the droplets, and as shown in Table 1, three distinct concentrations of oil 1%, 2.5%, and 5%, were considered for characterisation studies. The emulsion droplet's sizes grow larger as a result of the higher oil concentration.

In colloidal systems where the droplets are coated with emulsifiers, the *z*-average hydrodynamic diameter of the produced thyme nanodroplets exhibited a direct correlation with the size and structure of the emulsifier molecules. Different oil concentrations (1%, 2.5%, and 5%) were used to obtain various nanoemulsion concentrations and these formulations were exposed to different time intervals of sonication (10, 20, and 30 min). According to a first-order relationship, the reduction in particle size decreased with increasing "ultrasonication process time" (Table 1). The optimal ultrasonication process time is defined as the length of time required to achieve 99% of the "maximum attainable size reduction," which was found to be 10 min and was practically constant regardless of the process variables such as sample volume and ultrasonic amplitude [39]. Once a minimal particle size was achieved, there was no longer any noticeable reduction in particle size caused by ultrasonication; as shown in Table 1, sonication at 20 and 30 min increased the size droplet size and 10 min of sonication achieved the lowest droplet size. However, the polydispersity index was not obtained in the below 0.2-nm range. The PDI values around 0 indicate the maximum stability and the existence of monodispersed NEs. The lowest PDI values were obtained in 5% thyme nanoemulsion at 20 min of sonication.

Table 1 Characterisation of different thyme oil nanoemulsions based on their droplet size, polydispersity index, zeta potential, pH, and conductivity

Thyme NE (oil concentration)	Hydronamic size (d nm)	Polydispersity index	Zeta potential (mV)	pH	Conductivity (mS/cm)
Unsonicated (1%)	206.5 ± 2.82	0.338 ± 0.13	− 49.3 ± 1.01	6.34 ± 0.04	0.0428 ± 0.080
Unsonicated (2.5%)	269.3 ± 5.69	0.658 ± 0.14	− 54.60 ± 1.42	6.04 ± 0.03	0.0574 ± 0.097
Unsonicated (5%)	305.5 ± 29.7	0.377 ± 0.03	− 56.2 ± 3.27	5.78 ± 0.02	0.0699 ± 0.004
10-min sonication (1%)	54.48 ± 0.32	0.261 ± 0.005	− 43.3 ± 0.208	6.02 ± 0.01	0.0385 ± 0.0107
10-min sonication (2.5%)	118.0 ± 0.73	0.252 ± 0.003	− 40.40 ± 2.91	6.08 ± 0.04	00768 ± 0.0112
10-min sonication (5%)	119.1 ± 0.35	0.266 ± 0.003	− 43.60 ± 0.10	6.14 ± 0.12	0.0261 ± 0.0123
20-min sonication (1%)	166.8 ± 1.528	0.142 ± 0.018	− 36.6 ± 2.21	5.85 ± 0.03	0.0532 ± 0.0111
20-min sonication (2.5%)	140.9 ± 1.2	0.133 ± 0.019	− 43.3 ± 2.52	5.79 ± 0.05	0.0637 ± 0.0061
20-min sonication (5%)	122.2 ± 1.079	0.152 ± 0.009	− 36.8 ± 0.551	5.62 ± 0.01	0.0544 ± 0.0146
30-min sonication (1%)	364.9 ± 4.22	0.248 ± 0.01	− 12.3 ± 1.45	5.34 ± 0.01	0.169 ± 0.001
30-min sonication (2.5%)	215.4 ± 2.31	0.206 ± 0.003	− 13.5 ± 1.38	5.28 ± 0.02	0.173 ± 0.0023
30-min sonication (5%)	210.2 ± 1.81	0.225 ± 0.022	− 41.4 ± 0.79	5.17 ± 0.03	0.141 ± 0.0015

Zeta potential, which may also be used to determine the physical stability of NEs, is an indirect measurement of the electrical charge on the surface of droplets. High values of the zeta potential imply that the system is stabilised by repulsive forces between the droplets. Zeta potential is significant because the stability of colloidal dispersion is correlated with its value. A high zeta potential, whether negative or positive, often denotes good emulsion stability since it means that the particles will be maintained in the dispersed phase by their interaction with one another. When the absolute value of the sample's zeta potential is high enough ($\geq$20 mV), the repulsive force between the particles in the emulsion will be higher than the London force, and the sample will be stable. The thyme nanoemulsion (5%) when sonicated for 20 min showed PDI less than 0.2 which is an indication of monodisperse nanoemulsion formulation and exhibited the hydrodynamic size of 122.2 ± 1.079 nm and negatively high zeta potential of -36.8 mV. This formulation was considered ahead for stability check for 4 months and for heating-cooling cycles (as shown in Table 1). Monitoring the pH level is crucial for establishing the stability of the emulsions since fluctuations in pH signal the existence of chemical reactions that may degrade the final product's quality and there was not much variation in pH between all the formulations. The slight alteration in acidic pH as we increase the thyme oil concentration could be because of the presence of phenolic groups in the thyme oil. Due to the exterior phase of water in oil-in-water nanoemulsions, the nanoemulsions are highly conductive.

Stability of Nanoemulsion

Stress testing is necessary to rule out the potential of metastable formulations. Testing for thermodynamic stability on the nanoemulsions included centrifugation, a heating-cooling cycle, and freeze-thaw cycles. When there was no evidence of phase separation, turbidity, creaming, or cracking, they were considered to be passed. In comparison to regular emulsions, the nanoemulsion has a longer shelf life due to its thermodynamic stability. This sets them apart from emulsions with kinetic stability, which will ultimately phase-separate. By methodically evaluating *z*-averages, PDI, and zeta-potential up to 30 days at intervals of 5 days and ultimately after 3 months of storage, the stability of nanoemulsions at ambient temperature was also examined. Almost all the formulations passed these stability parameters (as shown in Table 2). Five percent of thyme oil NE (20-min sonication) did not show any phase separation at any step and was considered for stability check for 4 months. In comparison to other nanoemulsions, it demonstrated stability in terms of mean droplet size (157.1 ± 1.890 nm), PDI (0.086), and zeta-potential (-32 mV), as shown in Table 3. The average hydrodynamic size reduced in the second month and increased again in the third and fourth months; however, the PDI was constantly below 0.2. It was observed that the 5% nanoemulsion that was sonicated for 30 min was unstable like the unsonicated one and cannot be considered ahead. The biopolymers solutions' zeta potential, interfacial tension, and viscosity were often lowered throughout the sonication process, resulting in stable emulsions with lower droplet sizes. However, sonication for more than 20 min led to unstable nanoemulsions, which emphasises the importance of the duration of sonication.

Antibacterial Activity of Thyme Nanoemulsion

Despite several types of activities having been studied, it is still unknown exactly how nanoemulsion-based antimicrobial activity works. The hydrophobic impression of essential oil processes, which facilitate them to penetrate the cell film, aggravate the structure,

Table 2 Different thyme oil nanoemulsions were exposed to heating and cooling cycles, freeze–thaw cycles, and centrifugation to analyse the stability of all the listed formulations

Thyme NE (oil concentration)	Centrifuge	Heating-cooling cycle	Freeze thaw cycle	Inference
Unsonicated (1%)	−	−	−	Passed
Unsonicated (2.5%)	−	−	−	Passed
Unsonicated (5%)	−	−	+	Failed
10-min sonication (1%)	−	−	−	Passed
10-min sonication (2.5%)	−	−	−	Passed
10-min sonication (5%)	−	−	−	Passed
20-min sonication (1%)	−	−	−	Passed
20-min sonication (2.5%)	−	−	−	Passed
20-min sonication (5%)	−	−	−	Passed
30-min sonication (1%)	−	−	−	Passed
30-min sonication (2.5%)	−	−	−	Passed
30-min sonication (5%)	+	−	−	Failed

Table 3 The stability of 20-min sonication (5%) was measured for consecutive 4 months to observe the hydrodynamic size and polydispersity of NE to determine its stability

Thyme	1st month	2nd month	3rd month	4th month
Average size	122.2 ± 1.079	134 ± 0.007	157.7 ± 2.450	157.1 ± 1.890
PDI	0.152 ± 0.009	0.14 ± 0.06	0.078 ± 0.018	0.086 ± 0.019

and increase its permeability, is associated with a summed-up display. As a result of the increased permeability, there is the release of cell content, such as nucleic acids, amino acids, particles, and ATP. Different essential oils and blends of essential oils may respond differently to certain microorganisms. For instance, carvacrol, a substantial phenolic compound included in oregano and thyme oil, can damage the outer layer of several Gram-negative organisms, release endotoxins, and enhance the permeability of the film. Carvacrol was discovered to boost extracellular ATP levels while reducing intracellular ATP levels in research on *Escherichia coli (E. coli).*

Growth Inhibitory Activity

Essential oils include bioactive substances like terpenes and phenylpropenes. The composition, type, concentration, target microorganism, substrate composition, storage circumstances, and processing conditions all affect its antibacterial action. The lipid portion of the bilayer membrane is disturbed by these essential oil chemicals, particularly phenolic compounds, and their interactions with cell organelles can provide antibacterial activity. Thymol and carvacrol are the two main phenolic compounds in TEO that target the cytoplasmic membrane and change its structure and function, causing cell death, depending on the type of thyme plant. The cytoplasmic membrane being disrupted, which leads in

increased permeability and subsequent depolarisation, is the main mechanism for thymol and carvacrol.

Using growth inhibition experiments, the antibactericidal efficacy of thyme oil and nanoemulsion was examined. In *E. coli*, the thyme oil nanoemulsion showed the highest growth inhibition (88.46%) when compared to the control and the inhibition was equivalent to Triton X. This showed promising results to support the antibacterial effects of thyme nanoemulsion on *E. coli*. Similarly, for *B. subtilis* (57.1% growth inhibition) and *P. aeruginosa* (64.28% growth inhibition), thyme nanoemulsion showed significantly higher inhibition of growth compared to control and thyme oil. The bacterial growth inhibition was found the best for *S. aureus* (80% growth inhibition compared to control), showcasing significantly much more inhibition than the thyme oil and positive control Triton X (Fig. 1). The generated nanoemulsion and the extracted thyme essential oil had significantly different bactericidal effects, according to statistical analysis. The produced nanoemulsion's higher bactericidal activity may be attributed to their tiny particle size, which boosted the nanodroplet's surface-to-volume ratio and facilitated their adhesion to or penetration through membrane cells.

Determination of MIC and MBC

The lowest concentration of an antibacterial nanoemulsion that is bacteriostatic is known as the minimum inhibitory concentration (MIC) (inhibits the visible growth of bacteria). The lowest concentration of an antibacterial nanoemulsion necessary to eradicate germs during a predetermined time period is known as the minimum bactericidal concentration

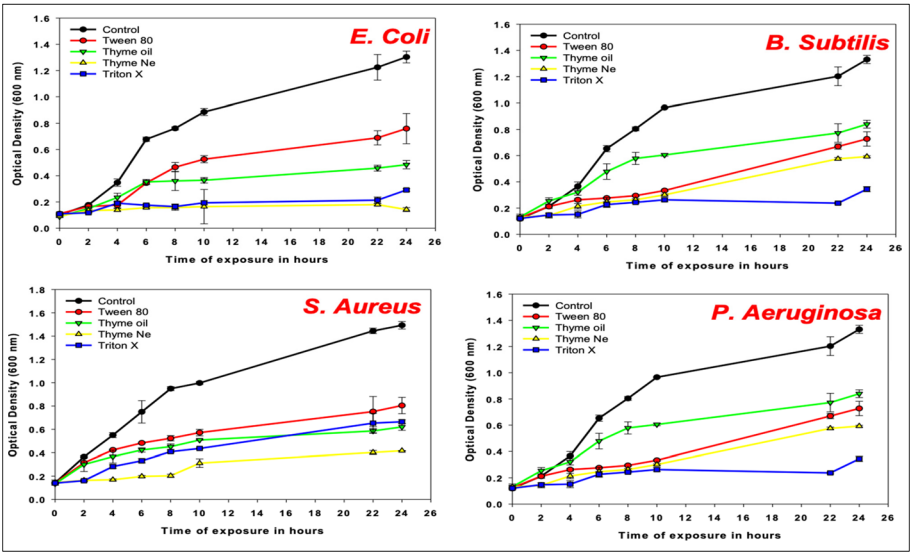

Fig. 1 The growth inhibitory activity for 24 h was observed in 4 bacterial species and when treated with thyme oil and thyme nanoemulsion. As a positive control, Triton X was utilised and Tween 80 was taken as a control to eliminate the effects mediated by it in the nanoemulsion. For *E. coli*, the thyme oil nanoemulsion showed the highest growth inhibition (88.46%) when compared to the control, followed by *S. aureus* exhibiting 80% growth inhibition, *B. subtilis* 57.1% growth inhibition, and *P. aeruginosa* 64.28% growth inhibition was observed

(MBC). The maximum dilution, MBC, exhibits a 99.9% reduction in the number of bacterial cells. To calculate the MIC in the nutrient broth, serial tenfold dilutions of a 5% thyme nanoemulsion with modified bacterial concentration were utilised. The control employed 1% Triton-X as a positive control and solely included inoculation broth. It was incubated for 24 h at 37 °C. The MIC endpoint is the thyme nanoemulsion concentration at which there is no discernible growth in the tubes. To verify the MIC values, the visual turbidity of the tubes was observed both before and after incubation. As shown in Table 4, in *S. aureus*, the dilution that inhibits bacterial growth (1:100) is also enough for killing the bacteria. However, for *E. coli*, *P. aeruginosa*, and *B. subtilis*, further 10 times dilution is required for bactericidal effect (MBC is 1:10 and MIC is 1:100). This result is concurrent with the growth inhibitory activity of nanoemulsion on *S. aureus.*

Viability Assay

The viability of *P. aeruginosa*, *E. coli*, *S. aureus*, and *B. subtilis* reduced significantly when the treatment of 5% thyme nanoemulsion was given in comparison to thyme oil (equivalent or more than the positive control). As live cells have an intact cell membrane, they exclude the Trypan blue dye, whereas dead cells uptake the dye. When compared to fenugreek nanoemulsion which is a known antibacterial, thyme nanoemulsion depicted similar antimicrobial properties, as shown in Fig. 2. Thyme nanoemulsion reduced the cell viability by 10%, 11%, 16%, and 37% in *E. coli*, *B. subtilis*, *S. aureus*, and *P. aeruginosa*, respectively, which is similar to the trend obtained when all 4 bacterial strains were treated with fenugreek nanoemulsion that is 10%, 17.5%, 10%, and 38% for *E. coli*, *B. subtilis*, *S. aureus*, and *P. aeruginosa*, respectively. However, thyme NE is more effective for *B. subtilis* compared to fenugreek NE (as shown in Fig. 2). Thyme nanoemulsion exhibits a much higher antibacterial activity against *P. aeruginosa* compared to Triton X. This is likely due to the fact that thyme nanoemulsion is more specific in its mode of action, targeting the bacterial cell membrane directly and causing less damage to other cell types. Additionally, the small particle size of the nanoemulsion allows for better penetration into the bacterial cell, increasing its effectiveness.

Membrane Permeability Assay

Numerous investigations have revealed that phytochemicals have a membrane-active mechanism that damages the membrane severely by rupturing its integrity [40]. Thyme essential

Table 4 The nanoemulsion demonstrated greater antibacterial efficacy against the four studied pathogens. For *B. subtilis*, *E. coli*, and *P. aeruginosa*, 1:10 dilution of thyme nanoemulsion was enough to be bactericidal; however, for *S. aureus*, even at a tenfold higher dilution of 1:100, 99.9% of the bacteria were eliminated. This depicts that even at a tenfold higher dilution, the thyme oil nanoemulsion shows a significant reduction in bacterial growth and also has bactericidal properties against *S. aureus*

Bacterial strains	MIC	MBC
E. coli	1:100	1:10
B. subtilis	1:100	1:10
S. aureus	1:100	1:100
P. aeruginosa	1:100	1:10

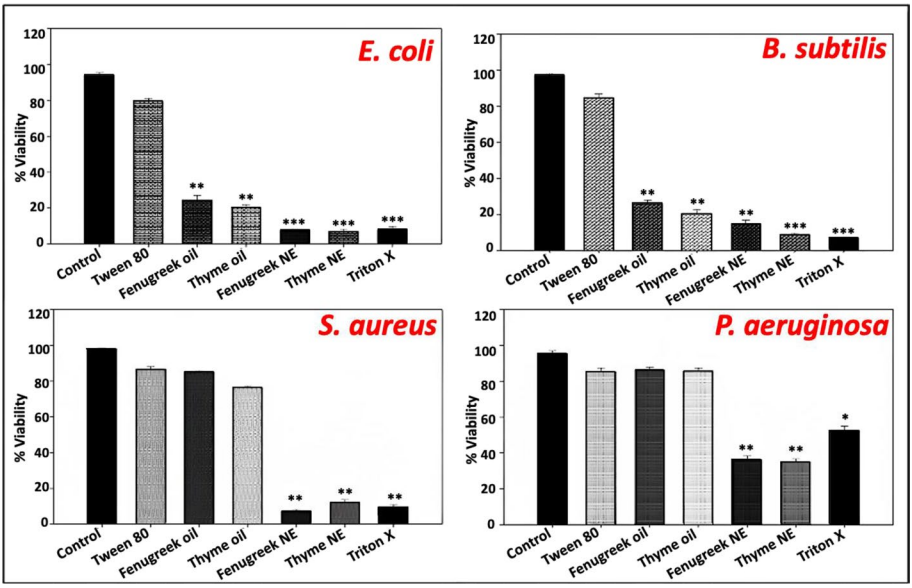

Fig. 2 Percent cell viability reduced significantly with the treatment of thyme nanoemulsion when compared to thyme oil. Thyme nanoemulsion reduced the cell viability by 10%, 11%, 16%, and 37% in *E. coli*, *B. subtilis*, *S. aureus*, and *P. aeruginosa*, respectively. A significant difference was observed between the cell viability when treated with thyme oil and thyme nanoemulsion in *S. aureus.* A 71% higher reduction in cell viability was observed in *S. aureus* when treated with thyme nanoemulsion, compared to thyme oil

oils include carvacrol, a phenolic monoterpenoid that affects the outer membrane but is thought to really act on the cytoplasmic membrane by causing passive ion transport across the membrane. According to a theory, cells exposed to carvacrol change the number of fatty acids in their membranes as a coping strategy to maintain ideal membrane shape and function. Carvacrol has been shown to have an effect on the Gram-negative bacteria's outer membrane. An increase in cell membrane leakage was observed when the bacterial cultures were treated with thyme nanoemulsion. The leakage in the cell membrane was observed to be more than the thyme oil and fenugreek controls (as shown in Fig. 3). This signifies that the thyme nanoemulsion disrupts the cell membrane integrity of all four strains of bacteria. At higher concentrations, thyme NE was more effective than fenugreek NE for *E. coli* and *P. aeruginosa*, that is 25% and 11% membrane permeability respectively. Fenugreek NE is known to display antibacterial efficacy against all microbes except *P. aeruginosa* in a range comparable to Ampillicin. Although *P. aeruginosa* is known to be resistant to Ampicillin, it was not resistant to the synthesised NE [36].

Anticancer Property of Thyme Nanoemulsion

Previous research has documented the protective effects of thyme oil and its main component, thymol, on liver damage, oxidative stress, inflammatory state, and apoptosis. To determine if the nanoemulsion improves the effectiveness of the thyme oil, the probable mechanism of the antitumorigenic nature of thyme nanoemulsion was examined and compared to thyme essential oil.

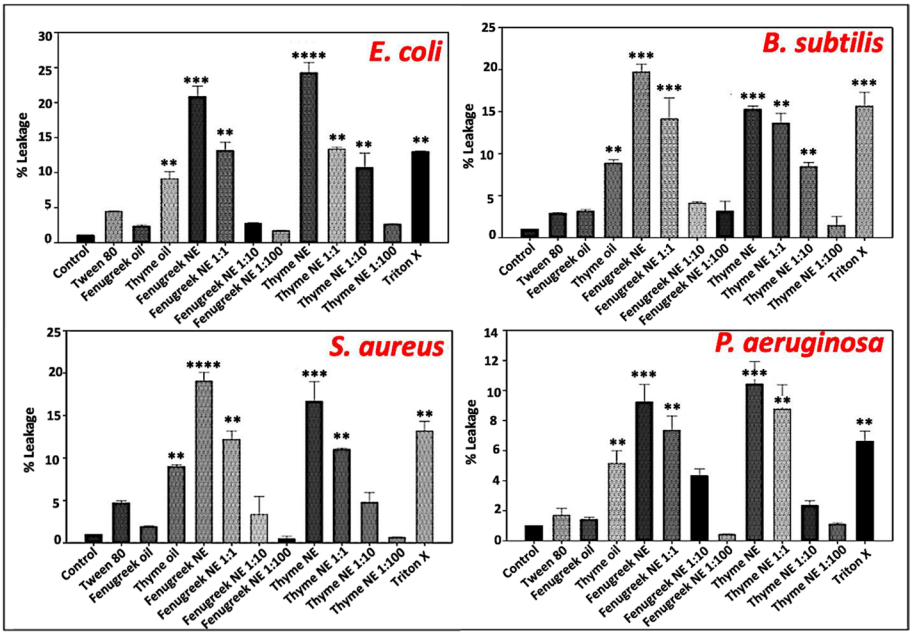

Fig. 3 The integrity of the cell membrane reduces with the increase in the concentration of thyme nanoemulsion and is more toxic to the strains compared to the controls. A cell membrane leakage of 25%, 15%, 17%, and 11% was observed in *E. coli*, *B. subtilis*, *S. aureus*, and *P. aeruginosa* respectively, after the treatment with thyme nanoemulsion

MTT Assay

The study advanced towards the evaluation of the cytotoxicity of the nanoemulsion on the human hepatocellular carcinoma cell line like Hep G2. The cells kept at the lowest concentration range of 25 µM for a longer duration of 24 h also exhibited cytotoxic properties in HepG2 cells. With an increase in concentration and duration of treatment, there is a significant decrease in cell viability. Tween 80 was taken as a vehicle control to eliminate the toxic effect generated by it that did not show any toxicity on the cells. The MTT assay demonstrated that the treatment with thyme nanoemulsion significantly affected cell viability after 24 h of exposure even at the lowest concentration of 25 µM, with a reduction of 28.33% of cell viability. Similarly, thyme nanoemulsion reduced by 8.8% Hep G2 viability after 6 h of exposure at 25 µM (as shown in Fig. 4). The maximum effects of thyme nanoemulsion were observed at 6 and 24 h of exposure at 400 µM (40.40% and 80% of cell viability reduction, respectively).

Cell Cycle Analysis

It is generally recognised that an unregulated cell cycle strongly relates to the development of cancer. The primary checkpoints in the cell cycle, G1 and G2, are crucial for the advancement of the cell cycle. Checkpoints in the cell cycle allowing the cell cycle to continue or to halt in reaction to DNA damage so that DNA repair may occur, which ensures proper DNA replication and division. The cell cycle DNA damage checkpoints prevent

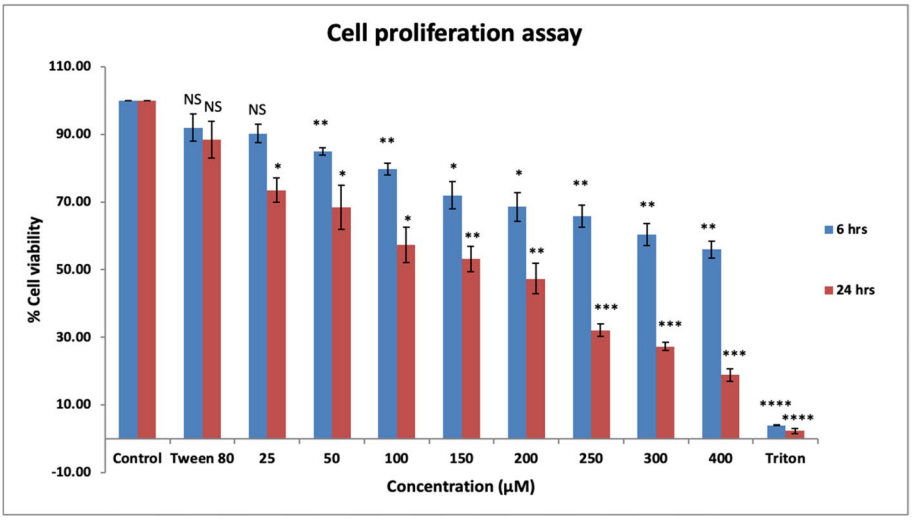

Fig. 4 Cell viability decreased with an increase in thyme nanoemulsion concentration and duration of treatment. The cell viability decreased by 50% at the concentration of 150 μM at 24 h of treatment. Similarly, at 400 μM of thyme nanoemulsion treatment, the cell viability reduced to less than 25%, strongly suggesting that the thyme nanoemulsion significantly influences the cell viability in concentration and time-dependent manner in HepG2 cells

entry into the S phase and mitosis, respectively, late in G1 and late in G2. The checkpoint control system is regulated by a family of protein kinases known as the Cdks2, which are in turn regulated by a wide range of proteins, including cyclins. The G2 checkpoint permits the cell to repair DNA damage before mitosis, much as the G1 checkpoint before the S phase. In fact, DNA damage may cause a more severe G2-M arrest in a cancer cell with a faulty G1 checkpoint. Numerous cellular processes are triggered by DNA damage, including the activation of Chk1, which phosphorylates and inactivates cdc25, resulting in the deactivation of the cdc2-B1 complex and G2-M arrest. Contrary to the theory that overcoming a checkpoint would cause a cell to enter apoptosis after experiencing first DNA damage, nanoscale emulsions have the ability to increase cytotoxicity in conjunction with greater checkpoint arrest [41]. To determine the kind of cell death caused by thyme nanoemulsion, flow cytometry and PI labelling were used to compute the fraction of cells in the sub-G1, G0/G1, S, and G2/M phases.

When a cell's DNA is harmed, the cell cycle is interrupted during the G2/M phase in order to give the damaged DNA time to be repaired. Among other regulatory proteins, the CDK1/cyclin B complex takes part in this checkpoint phase and controls cell passage through the G2/M phase. We found an unusual result by analysing the cell cycle: the thyme nanoemulsion blocked the passage from the G2/M phase, causing the cell cycle to stop there and perhaps undergo apoptosis. In light of this, it can be elucidated that thyme nanoemulsion causes arrest in cell cycle in hepatocarcinoma cells and may lead the cells to enter the apoptotic stage. The findings show that after 24 h of exposure, the treatment with thyme nanoemulsion significantly increased the fraction of cells that are halted in the G2/M cell cycle phase. This increase was dependent on concentrations. Compared to the control, more cells were delayed in the G2/M phase when exposed to thyme nanoemulsion. At the maximum thyme nanoemulsion concentration of 200 μM, the G2/M cell population increased from 18.08 to 24.30% in comparison to the control. Similarly, the percentage of G0/G1 cells

dropped from 67.98% in the control to 65.99% with the 200-µM treatment. This clearly shows that after being treated with thyme nanoemulsion, hepatocarcinoma cells are halted in the G2/M in the cell cycle and may even go through apoptosis (as shown in Fig. 5).

Gene Expression Studies Using RT-PCR

The by-products of regular cellular metabolism, or ROS, may be advantageous or detrimental based on their level and location of buildup. The endoplasmic reticulum (ER), the cytoplasm, and the mitochondria are the principal resources of ROS generated in the majority of mammalian cells. Three key signalling proteins are involved in the development of ER stress caused by abnormally high ROS levels which are PERK, ATF-6, and IRE1. The IRE1 protein is recognised to phosphorylate JNK, which regulates the production of mitochondrial indicators notably Bcl2, Bax, and Cytochrome C, resulting to caspase-mediated cell death [42]. As discussed in Figs. 6 and 7, the fold increase in Bax, Caspase 3, 8, and 9 along with a simultaneous decrease in BCL 2 indicates activation of both intrinsic and extrinsic pathways of apoptosis. When cells are treated with thyme nanoemulsion, survival indicators like Bcl-2 are less expressed, which reduces the inhibition of Bax and increases the expression of Bax (pro-apoptotic marker) (refer Figs. 6 and 7). As a result, the mitochondrial permeability transition pore, which allows cytochrome-c to enter the cytoplasm and form a heptamer-like structure with Apaf-1, continues to grow. Following the cleavage of pro-caspase-9 to caspase-9 and the formation of an apoptosome, this heptamer activates caspase-3 and caspase-7, causing apoptosis. The AIF escapes from mitochondria, moves to the nucleus, and aids in DNA damage that causes apoptosis.

The increase in gene expression levels of Apaf-1 and decrease in ERK suggest the activation of Apaf-induced apoptosis (as shown in Fig. 8). TNF-α and STAT 3 both are reported to have a dual role in cancer; however, in the present study, they both act as

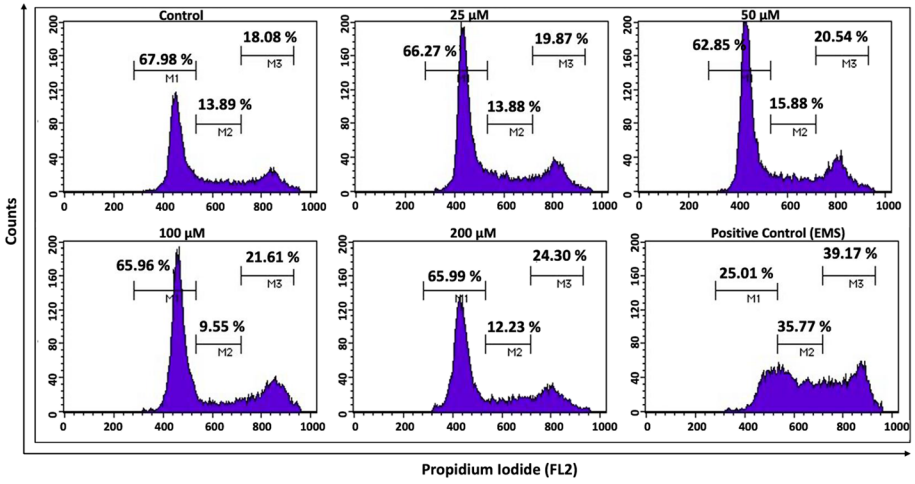

Fig. 5 Cells shift from G0/G1 to the G2/M gap phase and get arrested due to thyme nanoemulsion treatment in HepG2 cells. Compared to the control, the G2/M cell population increased from 18.08 to 24.30% in the highest concentration of 200 µM. Similarly, G0/G1 cell population decreased from 67.98% in the control and 65.99% in the treatment of 200 µM. This strongly suggests that the hepatocarcinoma cells get arrested in the G2/M stage of the cell cycle after the treatment of thyme nanoemulsion and maybe undergo apoptosis

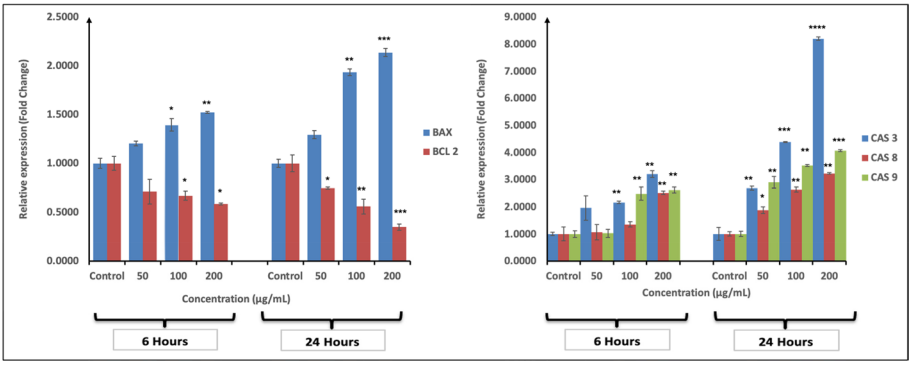

Fig. 6 Expression of genes involved in apoptosis. An increase in Bax, Caspase 3, 8, and 9 along with a simultaneous decrease in BcL-2 signifies the activation of both intrinsic and extrinsic pathways of apoptosis

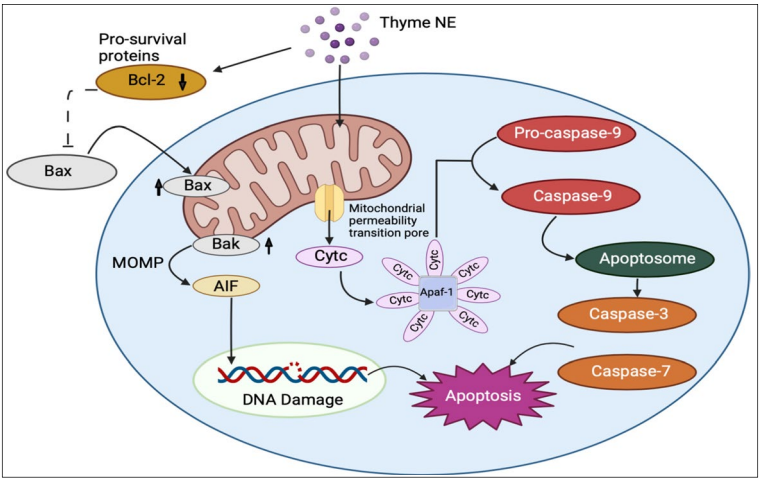

Fig. 7 A potential pathway for apoptosis due to thyme nanoemulsion treatment. Treatment with thyme nanoemulsion results in low expression of survival markers like Bcl-2 which in turn decreases the inhibition of Bax and there is a higher expression of Bax (pro-apoptotic marker). This subsequently progresses the development of mitochondrial permeability transition pore through which cytochrome-c is released into the cytoplasm and creates a heptamer-like structure with Apaf-1. This heptamer then cleaves pro-caspase-9 to caspase-9 and forms an apoptosome, stimulating caspase-3 and caspase-7 and resulting in apoptosis. The AIF is liberated from mitochondria, translocates to the nucleus, and contributes to DNA damage, leading to apoptosis

inducers of apoptosis. The increase in JNK represents the presence of ER stress which is associated with liver cancer. Cell cycle halt in the G2/M point is reflected by an upsurge in Cyclin B1 and a drop in P21. When treated for 6 h, there is an increase in H2AX level at a concentration of 50 µg/mL, which symbolises DNA repair; however, in the later concentration, there is a decrease in expression which suggests a lack of DNA repair. However, when treated for 24 h, there is a significant decrease in the level, suggesting no DNA repair at all. An increased level of iNOS suggests the generation of ROS (as shown in Fig. 8). The

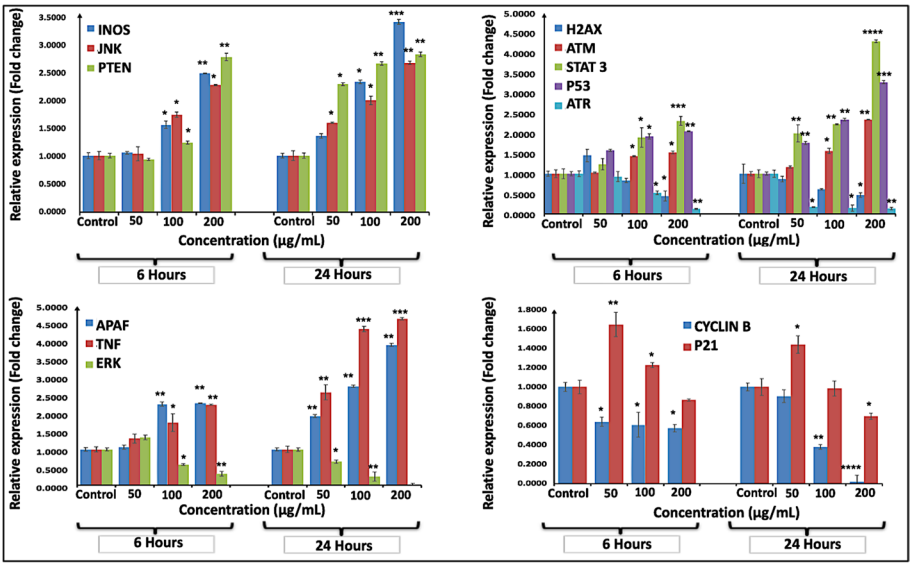

Fig. 8 Genes for ROS, MAPK, and ER stress pathway. A surge in JNK is associated with endoplasmic reticulum stress which results in a disturbance in the balance of the protein folding capacity to meet the demands of cells. A sharp decrease in H2AX level in laster concentrations represents a deficiency of DNA repair. An increased level of iNOS suggests the production of ROS. An increase in levels of PTEN and P53 levels suggests an increase in tumour suppression activities associated with different thyme nanoemulsion concentrations. Through their downstream targets, ATM and ATR kinases cause cell cycle arrest and allow DNA repair. An increase in Apaf-1 and a decrease in ERK imply the activation of Apaf-induced apoptosis. TNF-α and STAT 3 act as inducers of apoptosis in the present studies

thyme nanoemulsion might induce oxidative stress, which then decreases cyclin B1 and increases CdC2, which results in DNA damage and G2/M cell cycle arrest. The ATM and ATR kinases are activated by the availability of DNA double-strand defects or DNA replication stress, respectively. The main mechanism by which cell cycle progression is stopped is p53's phosphorylation in the presence of ATM and ATR. G1/S cell cycle arrest is largely caused by an increase in the cyclin-dependent kinase inhibitor p21, which is p53-dependent. DNA repair is lost when H2AX levels drop, and cell cycle arrest in the G2/M phase is responsible for a rise in Cyclin B1 and a reduction in P21 (as shown in Fig. 9).

Conclusion

Thyme nanoemulsion exhibited elevated bacterial growth inhibition, viability, and increased cell membrane permeability, compared to thyme oil, especially in *E. coli* and *B. subtilis*. Along with antimicrobial activity, thyme nanoemulsion exhibited anticancer properties by decreasing the viability of HepG2 hepatic cancer cells at even the lowest concentration of 25 µM when kept for 24 h. Cell cycle arrest in the G2/M phase, which is concomitant with cell cycle arrest seen in Fig. 6 with a rise in thyme nanoemulsion concentration, is demonstrated by a rise in Cyclin B1 and a reduction in P21. A drop in H2AX results in a lack of DNA repair. The antitumour effect was further confirmed in gene expression studies through RT-PCR that showed an increase in Bax, Caspase 3, 8, and 9 along with a

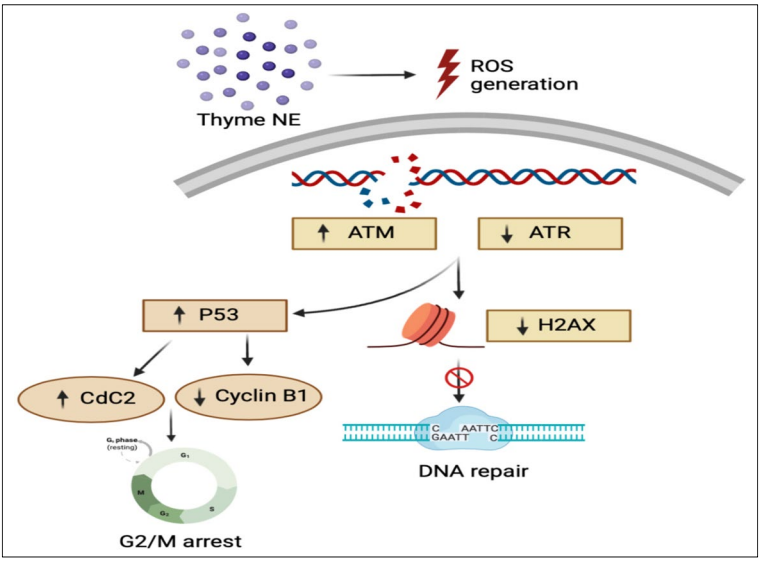

Fig. 9 DNA damage and cell cycle halt potential pathways. Increased oxidative stress brought on by thyme nanoemulsion causes a drop in cyclin B1 and a rise in CdC2, which causes cell-cycle halt t in the G2/M. DNA double-stranded breaks or DNA replication stress, respectively, activate the ATM and ATR kinases. The main mechanism by which cell cycle advancement is stopped is p53's phosphorylation in the presence of ATM and ATR. G1/S cell cycle arrest is largely caused by an increase in the cyclin-dependent kinase inhibitor p21, which is p53-dependent. DNA repair is lost when H2AX levels drop, and a cell cycle halt in the G2/M phase is responsible for a rise in Cyclin B1 and a drop in P21

simultaneous decrease in BcL 2 signifies the activation of both intrinsic and extrinsic pathways of apoptosis, along with a surge in gene expression levels of ROS, MAPK, and ER stress pathway. The increase in iNOS levels indicates the increase in ROS levels in cancer cells and a possible pathway for thyme nanoemulsion to target is either MAPK, ERK, and NF-KB pathways. This suggests that thyme nanoemulsion may have antioxidant capabilities, which may be investigated further in future research. Decreased expression of cH2AX, a sensitive biomarker of DNA double-strand breaks, also backed the observation that double-strand DNA breaks occurred. This alteration makes the DNA less compact, which may make room for the recruitment of proteins required for the repair of double-strand breaks. The double-strand breaks caused by the thyme nanoemulsion were unrepairable at the high dosage, as evidenced by a considerable drop in the expression of the cH2AX gene. The level of cH2AX was on the greater side at low dosage, indicating that this damage may be repaired by several repair enzymes. Cyclin B1, a regulatory protein engaged in mitosis, was also found to be declining. Future research might use this experiment as a baseline to examine the numerous pathways in which thyme nanoemulsion intervenes and its potential therapeutic effects.

Author Contribution All authors contributed to the study's conception and design. Nanoemulsion preparation, data collection, and analysis were performed by Simran Nasra. The first draft of the manuscript was written by Simran Nasra and all authors commented on previous versions of the manuscript. Analysis and manuscript review were performed by Nikita Meghani. Conceptualisation, supervision, funding acquisition, and writing—reviewing and editing were performed by Ashutosh Kumar. All authors read and approved the final manuscript.

Funding This work was supported by the Gujarat Institute for Chemical Technology (GICT) (AU/DBLS/GICT-nanomaterials/2016-17/01) for the funding and has been acknowledged for the establishment of a facility for environmental risk assessment of chemicals and nanomaterials.

Data Availability Data will be available on a reasonable request.

Declarations

Ethical Approval Not applicable

Consent to Participate Not applicable

Consent to Publish Not applicable

Competing Interests The authors declare no competing interests.

References

1. Pan, S.-Y., Litscher, G., Gao, S.-H., Zhou, S.-F., Yu, Z.-L., Chen, H.-Q., Zhang, S.-F., Tang, M.-K., Sun, J.-N., & Ko, K.-M. (2014). Historical perspective of traditional indigenous medical practices: The current renaissance and conservation of herbal resources. *Evidence-Based Complementary and Alternative Medicine*, *2014*, 20, Article ID 525340. https://doi.org/10.1155/2014/525340
2. Hileman, B. (2007). Food irradiation. *Chemical & Engineering News, 85*(3), 41–43.
3. El-Sayed, S. M., & El-Sayed, H. S. (2021). Antimicrobial nanoemulsion formulation based on thyme (Thymus vulgaris) essential oil for UF labneh preservation. *Journal of Materials Research and Technology, 10*, 1029–1041.
4. Sampaio, C. I., Bourbon, A. I., Gonçalves, C., Pastrana, L. M., Dias, A. M., & Cerqueira, M. A. (2022). Low energy nanoemulsions as carriers of thyme and lemon balm essential oils. *LWT, 154*, 112748.
5. Burt, S. (2004). Essential oils: Their antibacterial properties and potential applications in foods—A review. *International Journal of Food Microbiology, 94*(3), 223–53.
6. Bakkali, F., Averbeck, S., Averbeck, D., & Idaomar, M. (2008). Biological effects of essential oils–A review. *Food and Chemical Toxicology, 46*(2), 446–75.
7. Cosentino, S., Barra, A., Pisano, B., Cabizza, M., Pirisi, F. M., & Palmas, F. (2003). Composition and antimicrobial properties of Sardinian Juniperus essential oils against foodborne pathogens and spoilage microorganisms. *Journal of Food Protection, 66*(7), 1288–91.
8. Nielsen, C. K., Kjems, J., Mygind, T., Snabe, T., Schwarz, K., Serfert, Y., et al. (2017). Antimicrobial effect of emulsion-encapsulated isoeugenol against biofilms of food pathogens and spoilage bacteria. *International Journal of Food Microbiology, 242*, 7–12.
9. Carson, C. F., & Hammer, K. A. (2011). Chemistry and bioactivity of essential oils. *Lipids Essent Oils Antimicrob Agents, 25*, 203–238.
10. Peter, K. V. (2006). Handbook of herbs and spices: Volume 3: Woodhead publishing.
11. Siani, A., Ramos, Md. S., Menezes-de-Lima, O., Jr., Ribeiro-dos-Santos, R., Fernadez-Ferreira, E., Soares, R., et al. (1999). Evaluation of anti-inflammatory-related activity of essential oils from the leaves and resin of species of Protium. *Journal of Ethnopharmacology, 66*(1), 57–69.
12. Kowalczyk, A., Przychodna, M., Sopata, S., Bodalska, A., & Fecka, I. (2020). Thymol and thyme essential oil—New insights into selected therapeutic applications. *Molecules, 25*(18), 4125.
13. Hammoudi Halat, D., Krayem, M., Khaled, S., & Younes, S. (2022). A focused insight into thyme: Biological, chemical, and therapeutic properties of an indigenous Mediterranean herb. *Nutrients, 14*(10), 2104.
14. Kumari, S., Kumaraswamy, R., Choudhary, R. C., Sharma, S., Pal, A., Raliya, R., et al. (2018). Thymol nanoemulsion exhibits potential antibacterial activity against bacterial pustule disease and growth promotory effect on soybean. *Scientific Reports, 8*(1), 1–12.
15. Johny, A. K., Darre, M., Donoghue, A., Donoghue, D., & Venkitanarayanan, K. (2010). Antibacterial effect of trans-cinnamaldehyde, eugenol, carvacrol, and thymol on Salmonella Enteritidis and Campylobacter jejuni in chicken cecal contents in vitro. *Journal of Applied Poultry Research, 19*(3), 237–244.

16. Escobar, A., Perez, M., Romanelli, G., & Blustein, G. (2020). Thymol bioactivity: A review focusing on practical applications. *Arabian Journal of Chemistry, 13*(12), 9243–9269.
17. Liu, Q., Meng, X., Li, Y., Zhao, C.-N., Tang, G.-Y., & Li, H.-B. (2017). Antibacterial and antifungal activities of spices. *International Journal of Molecular Sciences, 18*(6), 1283.
18. Cai, C., Ma, R., Duan, M., & Lu, D. (2019). Preparation and antimicrobial activity of thyme essential oil microcapsules prepared with gum arabic. *RSC Advances, 9*(34), 19740–7.
19. Boskovic, M., Zdravkovic, N., Ivanovic, J., Djordjevic, J., Janjic, J., Pavlicevic, N., et al. (2016). Inhibitory effect of thyme and oregano essential oils and some essential oil components on Salmonella Senftenberg and Salmonella Give. *Scientific Journal "Meat Technology," 57*(1), 71–5.
20. Oliveira, M. MMd., Brugnera, D. F., & Piccoli, R. H. (2013). Essential oils of thyme and Rosemary in the control of Listeria monocytogenes in raw beef. *Brazilian Journal of Microbiology, 44*(4), 1181–1188.
21. Miladi, H., Slama, R., Mili, D., Zouari, S., Bakhrouf, A., & Ammar, E. (2013). Essential oil of *Thymus vulgaris* L. and *Rosmarinus officinalis* L.: Gas chromatography-mass spectrometry analysis, cytotoxicity and antioxidant properties and antibacterial activities against foodborne pathogens. *Natural Science*, *5*, 729–739. https://doi.org/10.4236/ns.2013.56090
22. Quendera, A. P., Barreto, A. S., & Semedo-Lemsaddek, T. (2019). Antimicrobial activity of essential oils against foodborne multidrug-resistant enterococci and aeromonads in planktonic and biofilm state. *Food Science and Technology International, 25*(2), 101–108.
23. Kuete, V. (2017). Thymus vulgaris. Medicinal spices and vegetables from Africa, 599–609.
24. Hayouni, E. A., Bouix, M., Abedrabba, M., Leveau, J.-Y., & Hamdi, M. (2008). Mechanism of action of Melaleuca armillaris (Sol. Ex Gaertu) Sm. essential oil on six LAB strains as assessed by multiparametric flow cytometry and automated microtiter-based assay. *Food Chemistry, 111*(3), 707–18.
25. Anton, N., Benoit, J.-P., & Saulnier, P. (2008). Design and production of nanoparticles formulated from nano-emulsion templates—A review. *Journal of Controlled Release, 128*(3), 185–99.
26. Chen, H., Zhang, Y., & Zhong, Q. (2015). Physical and antimicrobial properties of spray-dried zein–casein nanocapsules with co-encapsulated eugenol and thymol. *Journal of Food Engineering, 144*, 93–102.
27. El Asbahani, A., Miladi, K., Badri, W., Sala, M., Addi, E. A., Casabianca, H., et al. (2015). Essential oils: From extraction to encapsulation. *International Journal of Pharmaceutics, 483*(1–2), 220–43.
28. Donsì, F., Annunziata, M., Vincensi, M., & Ferrari, G. (2012). Design of nanoemulsion-based delivery systems of natural antimicrobials: Effect of the emulsifier. *Journal of Biotechnology, 159*(4), 342–50.
29. Rodríguez, J., Martín, M. J., Ruiz, M. A., & Clares, B. (2016). Current encapsulation strategies for bioactive oils: From alimentary to pharmaceutical perspectives. *Food Research International, 83*, 41–59.
30. Weiss, J., Gaysinsky, S., Davidson, M., McClements, J. (2009). Nanostructured encapsulation systems: Food antimicrobials. In *Global issues in food science and technology* (pp. 425–79). Elsevier.
31. Solans, C., Izquierdo, P., Nolla, J., Azemar, N., & Garcia-Celma, M. J. (2005). Nano-emulsions. *Current Opinion in Colloid & Interface Science, 10*(3–4), 102–10.
32. Sharifi-Rad, M., Varoni, E. M., Iriti, M., Martorell, M., Setzer, W. N., del Mar, C. M., et al. (2018). Carvacrol and human health: A comprehensive review. *Phytotherapy Research, 32*(9), 1675–1687.
33. Islam, M. T., Khalipha, A. B., Bagchi, R., Mondal, M., Smrity, S. Z., Uddin, S. J., et al. (2019). Anticancer activity of Thymol: A literature-based review and docking study with emphasis on its anticancer mechanisms. *IUBMB Life, 71*(1), 9–19.
34. Nagoor Meeran, M. F., Javed, H., Al Taee, H., Azimullah, S., & Ojha, S. K. (2017). Pharmacological properties and molecular mechanisms of thymol: Prospects for its therapeutic potential and pharmaceutical development. *Frontiers in Pharmacology, 8*, 380.
35. Ahmad, A., Saeed, M., & Ansari, I. A. (2021). Molecular insights on chemopreventive and anticancer potential of carvacrol: Implications from solid carcinomas. *Journal of Food Biochemistry, 45*(12), e14010.
36. Mansuri, A., Chaudhari, R., Nasra, S., Meghani, N., Ranjan, S., & Kumar, A. (2023). Development of food-grade antimicrobials of fenugreek oil nanoemulsion—Bioactivity and toxicity analysis. *Environmental Science and Pollution Research, 30*(10), 24907–24918.
37. Meghani, N., Patel, P., Kansara, K., Ranjan, S., Dasgupta, N., Ramalingam, C., et al. (2018). Formulation of vitamin D encapsulated cinnamon oil nanoemulsion: Its potential anti-cancerous activity in human alveolar carcinoma cells. *Colloids and Surfaces B: Biointerfaces, 166*, 349–357.
38. Moghimi, R., Ghaderi, L., Rafati, H., Aliahmadi, A., & McClements, D. J. (2016). Superior antibacterial activity of nanoemulsion of Thymus daenensis essential oil against E. coli. *Food Chemistry, 194*, 410–5.
39. Pratap-Singh, A., Guo, Y., Lara Ochoa, S., Fathordoobady, F., & Singh, A. (2021). Optimal ultrasonication process time remains constant for a specific nanoemulsion size reduction system. *Scientific Reports, 11*(1), 1–12.

40. Khameneh, B., Eskin, N. M., Iranshahy, M., & Fazly Bazzaz, B. S. (2021). Phytochemicals: A promising weapon in the arsenal against antibiotic-resistant bacteria. *Antibiotics, 10*(9), 1044.
41. DiPaola, R. S. (2002). To arrest or not to G2-M Cell-cycle arrest: Commentary re: AK Tyagi et al., Silibinin strongly synergizes human prostate carcinoma DU145 cells to doxorubicin-induced growth inhibition, G2-M arrest, and apoptosis. Clin. Cancer Res., 8: 3512–3519, 2002. *Clinical Cancer Research, 8*(11), 3311–3314.
42. Lambert, R., Skandamis, P. N., Coote, P. J., & Nychas, G. J. (2001). A study of the minimum inhibitory concentration and mode of action of oregano essential oil, thymol and carvacrol. *Journal of Applied Microbiology, 91*(3), 453–62.